Frontiers in Bioscience Landmark

Front. Biosci. (Landmark Ed) **2026**; 31(11): 52450
https://doi.org/10.31083/FBL52450

Original Research

Xinmailong Attenuates Sepsis-Induced Myocardial Dysfunction via HO-1-Mediated Regulation of Autophagy and Pyroptosis

Yuan Tian[1,2,3], Wen Xiao[1,2], Yanjuan Liu[1,2], Shiyu Liao[1,2,3], Ting Cheng[1,2], Xiaoxiao Gu[1,2], Yu Jiang[1,2], Lili Yuan[3,*], Yuanzhu Xie[1,2,*]

[1]Institute of Emergency Medicine, The First Affiliated Hospital of Hunan Normal University (Hunan Provincial People's Hospital), 410005 Changsha, Hunan, China
[2]Hunan Provincial Key Laboratory of Emergency and Critical Care Metabonomics, 410005 Changsha, Hunan, China
[3]Department of Cardiovascular Medicine, Hunan Second People's Hospital (Hunan Provincial Brain Hospital), 410007 Changsha, Hunan, China
*Correspondence: shushu622@qq.com (Lili Yuan); yuanzhuxie@hunnu.edu.cn (Yuanzhu Xie)
Academic Editor: Ioanna-Katerina Aggeli
Submitted: 31 March 2026 Revised: 2 July 2026 Accepted: 7 July 2026 Published: 16 November 2026

Abstract

Background: Sepsis-induced myocardial dysfunction (SIMD) is a serious and life-threatening complication. It is clinically vital to elucidate the pathogenic mechanisms of SIMD and identify promising therapeutic interventions. This study aimed to investigate the cardioprotective mechanism of Xinmailong (XML) injection against SIMD by regulating autophagy and pyroptosis via heme oxygenase-1 (HO-1) activation. **Methods:** SIMD was induced by lipopolysaccharide (LPS) in animal and cell models. Echocardiography, enzyme-linked immunosorbent assay (ELISA), and hematoxylin and eosin (H&E) staining were used to assess cardiac function. The expression of HO-1, autophagy-related, and pyroptosis-related proteins was measured by Western blot and immunofluorescence. **Results:** XML treatment decreased mortality rates in mice with SIMD while also reducing myocardial damage. The biochemical indicators of myocardial damage, creatine kinase and lactate dehydrogenase, were significantly reduced after XML treatment. The expression of HO-1 and LC3-II/I were upregulated, whereas NLRP3, cleaved caspase-1, ASC, and gasdermin D (GSDMD) were downregulated after XML treatment. Compared with LPS-treated cells, XML treatment significantly inhibited pyroptosis and increased autophagy in HL-1 cells. These protective effects were reversed by the HO-1 inhibitor zinc protoporphyrin (ZnPP) and the autophagy inhibitor 3-MA. **Conclusion:** XML alleviates LPS-induced SIMD via HO-1 activation, reducing reactive oxygen species (ROS) generation and oxidative stress, inhibiting NLRP3 inflammasome-mediated pyroptosis, and restoring autophagy.

Keywords: myocardial injury; pyroptosis; apoptosis; sepsis; cardiomyopathies

1. Introduction

Sepsis is a serious medical condition characterized by systemic organ failure resulting from an uncontrolled immune response to pathogen invasion. It is one of the major public health problems worldwide, with a high mortality rate [1]. Sepsis-induced myocardial dysfunction (SIMD) is a common complication of sepsis, characterized by impaired cardiac contractility and ventricular dilation [2]. The pathogenesis of SIMD involves inflammatory responses, oxidative stress, and cell death, including pyroptosis and apoptosis. Despite extensive research, the exact mechanisms underlying SIMD remain incompletely understood, and effective therapeutic strategies are still lacking [3].

NLRP3-mediated pyroptosis plays a critical role in the inflammatory process during sepsis, strengthening inflammatory responses and exacerbating tissue damage [4,5]. The NLRP3 inflammasome requires priming and activation signals, leading to the assembly of the inflammasome complex and the activation of caspase-1 [6,7]. Activated caspase-1 cleaves gasdermin D (GSDMD), forming pores in the cell membrane and releasing pro-inflammatory cytokines such as IL-1β and IL-18 [8,9]. In the context of sepsis, the NLRP3 inflammasome activation in cardiomyocytes contributes to myocardial injury and dysfunction, making it a potential therapeutic target for SIMD.

Xinmailong (XML) is extracted from the *Periplaneta americana* and contains various bioactive compounds, including peptides, amino acids, and polysaccharides [10,11]. It is an officially approved traditional Chinese medicinal injection in China (National Medical Approval No. Z20060443) and is clinically authorized as an adjuvant therapy for chronic congestive heart failure and ischemic heart disease. Previous studies have demonstrated that XML exhibits cardioprotective effects, including anti-inflammatory, antioxidant, and anti-apoptotic properties [10,12,13]. However, the specific mechanisms by which XML exerts its protective effects in SIMD remain unclear [14]. Therefore, this study aimed to investigate the protective effects of XML on lipopolysaccharide (LPS)-induced myocardial dysfunction and to explore the underlying mechanisms, particularly focusing on the regulation of heme oxygenase-1 (HO-1)-mediated autophagy and pyroptosis.

Copyright: © 2026 The Author(s). Published by IMR Press.
This is an open access article under the CC BY 4.0 license.

Publisher's Note: IMR Press stays neutral with regard to jurisdictional claims in published maps and institutional affiliations.

2. Methods

2.1 Animals

Eight- to ten-week-old male C57BL/6 mice were purchased from Hunan SJA Laboratory Animal Company (Hunan Province, certification number SCXK 2019-0004). All procedures were performed in the animal facility of Hunan Provincial People's Hospital after 7 days of acclimatisation. All mice were housed under standard conditions (23 ± 2 °C) with a 12-hour light/dark cycle and free access to food and water. At the end of the experiments, all mice were euthanized by cervical dislocation under deep anesthesia (inhaled 2% isoflurane) to minimize suffering. All animal experiments were approved by the Institutional Animal Care and Use Committee in Hunan Provincial People's Hospital (Approval Number No. 69/2023). Notably, unless otherwise specified in the figure legends, all "n" values reported in this study represent biological replicates, which were derived from independent breeding batches and processed on separate experimental days to ensure reproducibility and minimize batch effects. Mice were randomly assigned to different groups using a computer-generated random number table, and all outcome measurements were performed by investigators blinded to the group allocation. Ten additional mice per group were included to account for potential death. To induce septic cardiac dysfunction, the mice received an intraperitoneal injection of LPS (10 mg/kg) as described previously [15]. XML pretreatment was performed 6 hours prior to LPS challenge via daily intraperitoneal injection. The murine XML dose of 50 mg/kg/day was calculated from the clinical adult dose of 5 mg/kg/day using the Meeh-Rubner allometric scaling formula, which is further supported by available pharmacological evidence and ensures rational dose conversion and good clinical translational relevance for this preclinical study [11].

2.2 Materials

XML (No. 2102109, Tengchong, Yunnan, China) was obtained from Yunnan Tengchong Pharmaceutical Company. LPS (L2880, Sigma-Aldrich, St. Louis, MO, USA) was purchased from Sigma-Aldrich. Kits for the detection of creatine kinase (CK, A032-1-1) and lactate dehydrogenase (LDH, A020-2-2) were purchased from Elabscience Biotechnology Co., Ltd. (Wuhan, Hubei, China). Interleukin-1β (IL-1β, EK201B) and Interleukin-18 (IL-18, EK218) were purchased from MultiSciences (Lianke) Biotech Co., Ltd., Hangzhou, Zhejiang, China. Dihydroethidium (DHE, BL762A) was purchased from Biosharp (Hefei, Anhui, China).

2.3 Echocardiographic Assessment

At 24 hours post-LPS, the mice were anesthetized with 2% isoflurane (Jiangsu Zhongmu Beikang Pharmaceutical Co., Ltd., Taizhou, Jiangsu, China), and their chest hair was removed. The evaluation of cardiac performance was carried out with a mobile veterinary ultrasound device (S7 Sci, Mindray Animal Medical, Shenzhen, China) with a 30 Hz probe, by using M-mode recordings to measure the size of the left ventricle in both systole and diastole.

2.4 Biochemical Analysis

Blood samples were collected at the corresponding time intervals after the pharmacological interventions for biochemical analysis. Analyses were performed according to the manufacturer's protocol using kits for the detection of CK and LDH.

2.5 Hematoxylin-Eosin (H&E) Staining

Cardiac tissues were processed for H&E staining following standard histological protocols [16]. After fixation in 4% paraformaldehyde overnight at 4 °C, the specimens were embedded in paraffin and sliced into 5-μm sections. The sections were then deparaffinized, rehydrated, and stained with H&E. Microscopic images were captured using a digital camera attached to an Olympus microscope.

2.6 Cell Culture and Treatment

The HL-1 cell line (AW-CNM080) was purchased from the Changsha Abiowell Biotechnology Co., Ltd., and cells at passage 8 were used throughout the study. The cells were cultured in DMEM high glucose medium (GNM12800-L, GENOM Biotech, Hangzhou, China) supplemented with 10% fetal bovine serum (FBS) (GNMFBCS5, GENOM Biotech, Hangzhou, China) and 1% penicillin-streptomycin in an incubator at 37 °C with 5% CO_2. The HL-1 cells were stimulated with LPS (1 μg/mL) for 24 hours to establish the cellular damage model, and the cells were pretreated with XML for 6 hours before the LPS challenge. To further explore the underlying mechanisms, cells were pretreated with 3-methyladenine [17] (3-MA, 5 mM, S2767, Selleck Chemicals LLC, Houston, TX, USA) for 1 hour or zinc protoporphyrin [18] (ZnPP, 10 μM, HY-101193, MedChemExpress LLC, Monmouth Junction, NJ, USA) for 6 hours before LPS treatment. The cell lines were validated by STR profiling and tested negative for mycoplasma.

2.7 Cell Viability Assay

Cell viability was assessed using the CCK-8 assay. HL-1 cells were seeded into 96-well plates at a density of 3×10^3 cells per well. To determine the non-toxic concentration range of XML, HL-1 cells were treated with XML for 24 hours. CCK-8 solution (10 μL, BL1055A, Biosharp, Hefei, China) was then added to each well for 1 hour at 37 °C, and absorbance was measured at 450 nm.

2.8 Western Blot Analysis

The cardiac tissue samples were cryopreserved, and proteins were subsequently extracted from the tissue with RIPA buffer (BL504A, Biosharp, Hefei, China) supplemented with protease and phosphatase inhibitor cocktails.

Equal amounts of protein were separated by SDS-PAGE and transferred onto PVDF membranes. Membranes were blocked with 5% non-fat milk for 1 hour and then incubated with primary antibodies overnight at 4 °C. After washing, membranes were incubated with secondary antibodies for 1 hour at room temperature. Protein bands were visualized using ECL reagent (BL520B, Biosharp, Hefei, China) and visualized with a ChemiDoc™ Imaging System (Bio-Rad Laboratories, Inc., Hercules, CA, USA). Primary antibodies against NLRP3 (R381207, 1:1000, Chengdu Zen Bioscience Co., Ltd., Chengdu, Sichuan, China), ASC (67824T, 1:1000, Cell Signaling Technology, Danvers, MA, USA), cleaved caspase-1 (341030, 1:1000, Chengdu Zen Bioscience Co., Ltd., Chengdu, Sichuan, China), GSDMD (AF4012, 1:1000, Affinity Biosciences, Changzhou, Jiangsu, China), LC3B (R381544, 1:1000, Chengdu Zen Bioscience Co., Ltd., Chengdu, Sichuan, China), HO-1 (ab68477, 1:1000, Abcam Shanghai Trading Co., Ltd., Shanghai, China), SQSTM1/P62 (R380612, 1:1000, Chengdu Zen Bioscience Co., Ltd., Chengdu, Sichuan, China), GAPDH (AB0037, 1:5000, Abways Co., Ltd., Shanghai, China), and the rabbit anti-goat HRP secondary antibody (511203, 1:10,000, Chengdu Zen Bioscience Co., Ltd., Chengdu, Sichuan, China) were used.

2.9 Flow Cytometry

Flow cytometric data were analyzed using FlowJo. After excluding debris and cell aggregates based on FSC/SSC and FSC-A/FSC-H doublet discrimination, the mean fluorescence intensity (MFI) of DHE in the PE channel was measured to evaluate intracellular ROS levels. Cells were plated in 6-well plates at a density of 10^6 cells per well and allowed to grow for 24 hours. After the different experimental treatments, cells were transferred to centrifuge tubes and washed with PBS. DHE was prepared as a 1:4000 dilution in serum-free medium. A 1 mL aliquot solution was applied to each sample, which was then incubated for 40 minutes under respective culture conditions. After three centrifugal washes with serum-free medium, cells were resuspended in 500 µL PBS and preserved on ice prior to flow cytometry.

2.10 Immunofluorescence Analysis

Cells were cultured in 6-well plates and fixed with 4% paraformaldehyde solution at room temperature for 15 minutes. Cell membranes were then permeabilized with 0.5% Triton X-100 (P0096, Beyotime Biotech Inc., Shanghai, China) for 15 minutes. After two rounds of PBS washing, samples were incubated with 3% goat serum at room temperature for 30 min to block non-specific binding. Primary antibodies were applied to the specimens for immunostaining for 60 minutes. Then, secondary antibodies labeled with Cy3 or FITC fluorophores were applied to the samples for 30 minutes under light-protected conditions. The last step was examination of nuclear structures by staining with the fluorescent DNA-binding compound DAPI.

2.11 Statistical Analysis

Data are presented as mean ± standard deviation (SD) from at least three independent experiments. Statistical analysis was performed using SPSS 26.0 (IBM Corp., Chicago, IL, USA) and GraphPad Prism 9.0.0 (Boston, MA, USA). One-way ANOVA followed by Tukey's post hoc test was used for comparisons among multiple groups. $p < 0.05$ was considered statistically significant.

3. Results

3.1 XML Ameliorated LPS-Induced Myocardial Injury and Dysfunction

To investigate the effect of XML on LPS-induced cardiac injury, mice were pretreated with XML for 6 hours and subsequently challenged with LPS. Survival was monitored at 3, 6, 12, 24, 36, 48 and 72 hours after LPS challenge. The results showed that the survival rate in the LPS group was significantly lower compared to the control group, whereas XML pretreatment significantly improved survival (Fig. 1A). Echocardiography revealed that the LPS group had decreased left ventricular ejection fraction (LVEF) and fractional shortening (LVFS), while serum levels of lactate dehydrogenase (LDH) and creatine kinase (CK) were markedly elevated. Notably, XML treatment effectively alleviated both the cardiac dysfunction and the elevation of these injury biomarkers (Fig. 1B,C). In myocardial sections from control animals, the tissue architecture appeared normal, with regularly arranged myocardial fibers and no obvious morphological abnormalities. In contrast, at 24 hours after LPS administration, cardiac tissues exhibited evident structural disarray, characterized by loosely and irregularly arranged myocardial fibers, altered cardiomyocyte morphology with enlarged intercellular spaces. However, these LPS-induced histopathological changes were markedly attenuated by XML pretreatment. The H&E results are shown in Fig. 1D. Those observations indicate that XML can ameliorate LPS-mediated cardiac functional impairment in mice.

3.2 XML Promotes Autophagy and Alleviates Sepsis-Induced Myocardial Dysfunction in Mice via HO-1

HO-1 plays a critical role in attenuating oxidative damage induced by LPS and maintaining cellular homeostasis, particularly in cardiac tissue [19]. Therefore, we investigated whether the cardioprotective effect of XML is related to HO-1 in the SIMD model. Western blot and immunofluorescence results showed that HO-1 expression was upregulated in the presence of XML in cardiac tissue (Fig. 2A–C).

To determine whether XML attenuates LPS-induced cardiac injury by suppressing pyroptosis, we examined the expression of GSDMD, caspase-1, ASC, and NLRP3 by Western blot. Both tissue and blood samples were collected, and the expression of pyroptosis-associated proteins and inflammatory cytokine secretion were assessed by Western

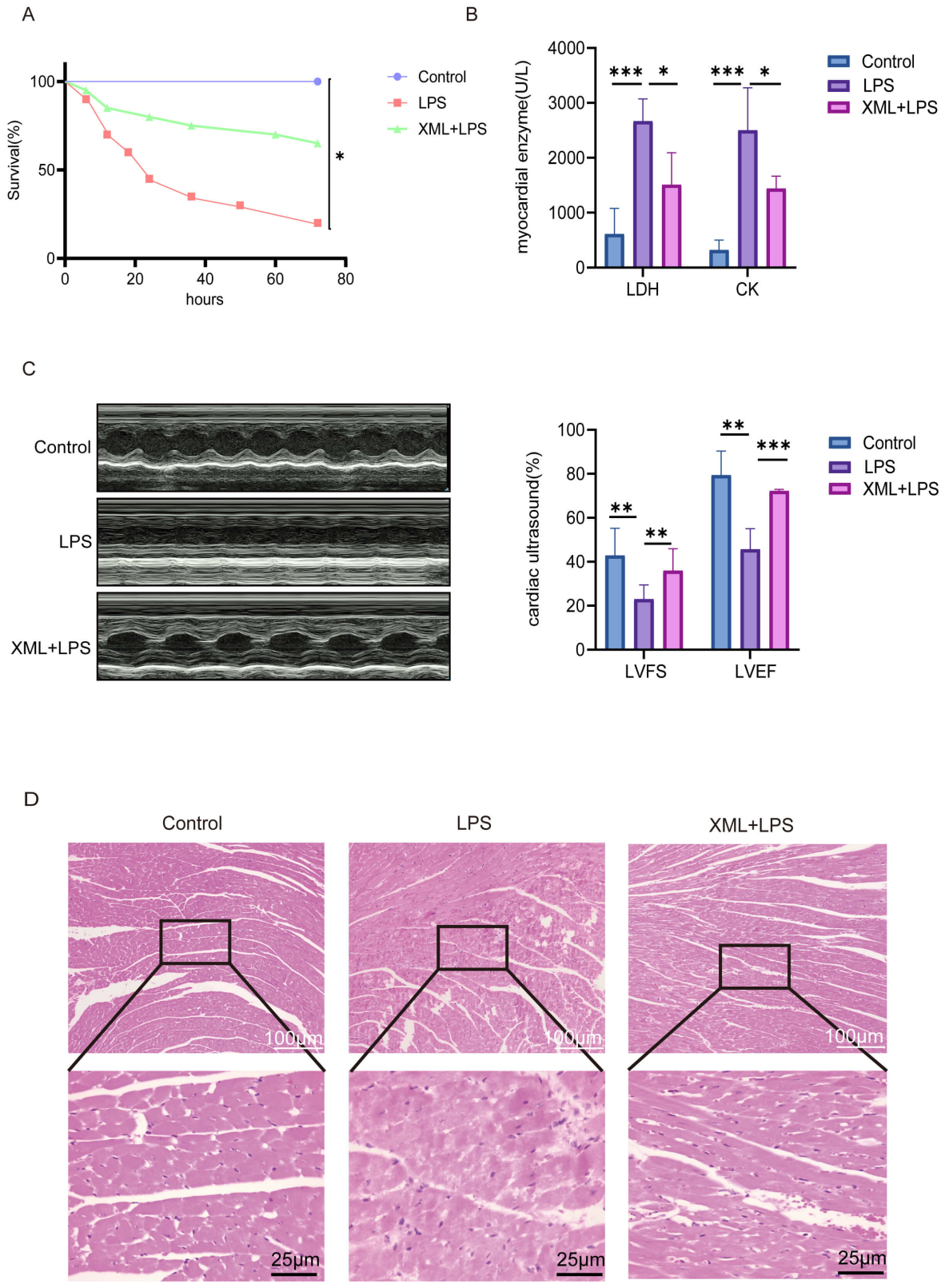


Fig. 1. Protective effect of XML on SIMD mice. (A) Survival curves of mice in each group (n = 20, biological duplications). (B) Detection of myocardial enzyme levels (n = 8). (C) Detection of cardiac function LVEF and LVFS indicators (n = 8). (D) H&E staining of myocardial tissues (n = 3) (scale bar: 100 μm/25 μm). LPS, Lipopolysaccharide; XML, Xinmailong; SIMD, Sepsis-induced myocardial dysfunction; H&E, hematoxylin/eosin; LVEF, left ventricular ejection fraction; LVFS, left ventricular fractional shortening. $^{*}p < 0.05$, $^{**}p < 0.01$, $^{***}p < 0.001$.

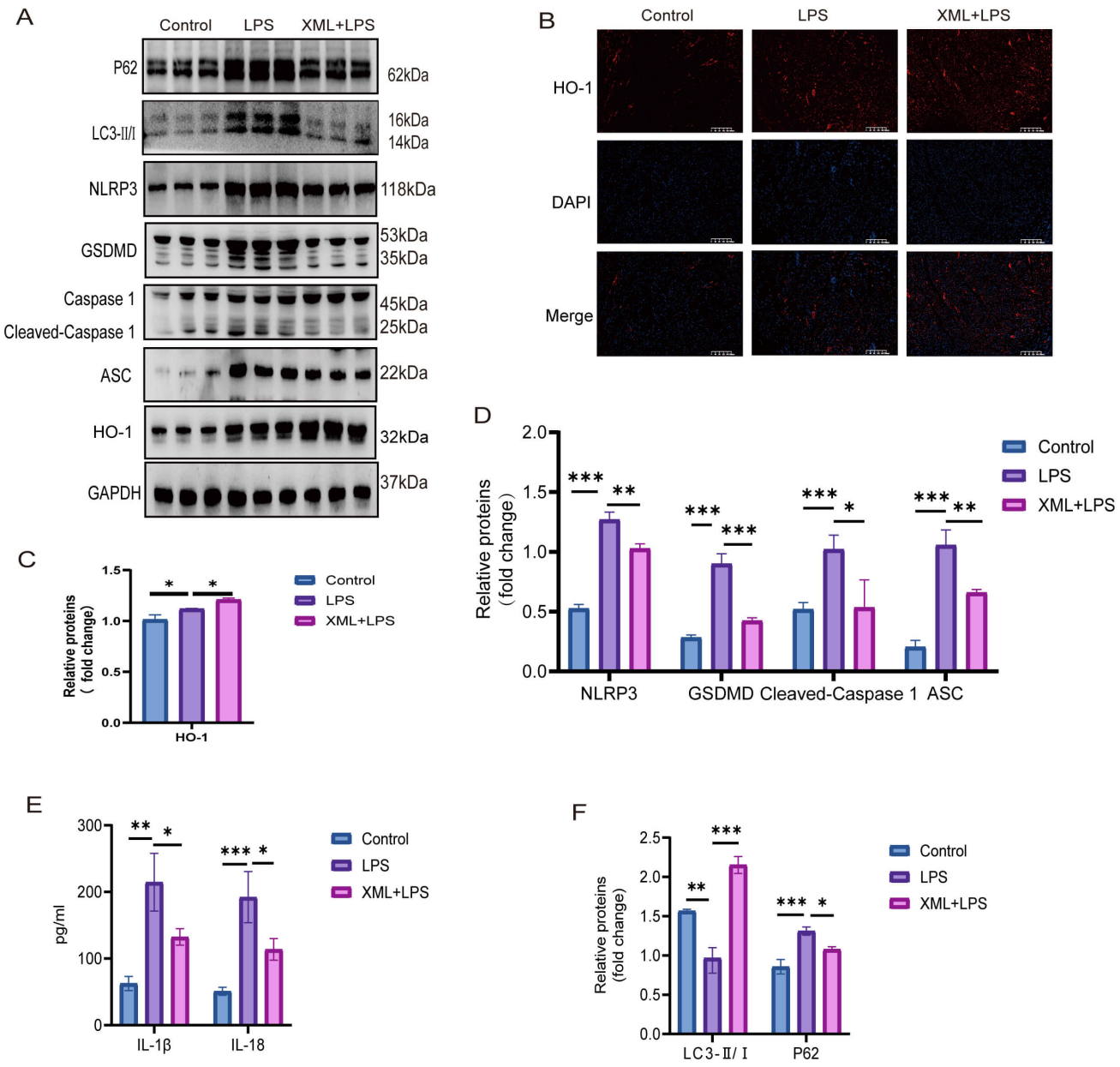


Fig. 2. XML alleviated mice's SIMD and promoted autophagy by regulating HO-1. (A) The expression of HO-1, and inflammasome-related proteins (NLRP3, GSDMD, cleaved caspase-1, ASC) associated with pyroptosis was determined by Western blot. (B) The expression of HO-1 in myocardial tissue was assessed using immunofluorescence analyses (scale bar: 200 μm). (C,D) The protein levels were quantified and normalized to GAPDH. (E) Additionally, ELISA was used to detect inflammatory cytokines IL-1β and IL-18 in mouse serum (n = 6). (F) The expression levels of autophagy-related proteins LC3-II/I and P62 were quantified, with GAPDH as the internal reference for normalization (n = 6). $^{*}p < 0.05$, $^{**}p < 0.01$, $^{***}p < 0.001$. HO-1, heme oxygenase-1; GAPDH, Glyceraldehyde-3-phosphate dehydrogenase; NLRP3, NLR family pyrin domain containing 3; GSDMD, gasdermin D; ASC, Apoptosis-associated speck-like protein containing a CARD; ELISA, enzyme-linked immunosorbent assay; IL-1β, Interleukin-1 beta; LC3-II, Microtubule-associated protein 1 light chain 3-II.

blot and ELISA, respectively. The results showed that GSDMD, caspase-1, ASC, and NLRP3 were significantly upregulated in the myocardial tissue of LPS-treated mice (Fig. 2A,D). Enzyme-linked immunosorbent assay (ELISA) results also showed that IL-18 and IL-1β concentrations were markedly elevated in the LPS group (Fig. 2E). These results indicate that the cardioprotective effect of XML against LPS-induced damage may be mediated by suppressing the pyroptotic pathway in myocardial cells.

Autophagy is crucial for maintaining cellular homeostasis; however, its precise role in LPS-induced myocardial injury has not been fully elucidated [20]. To explore

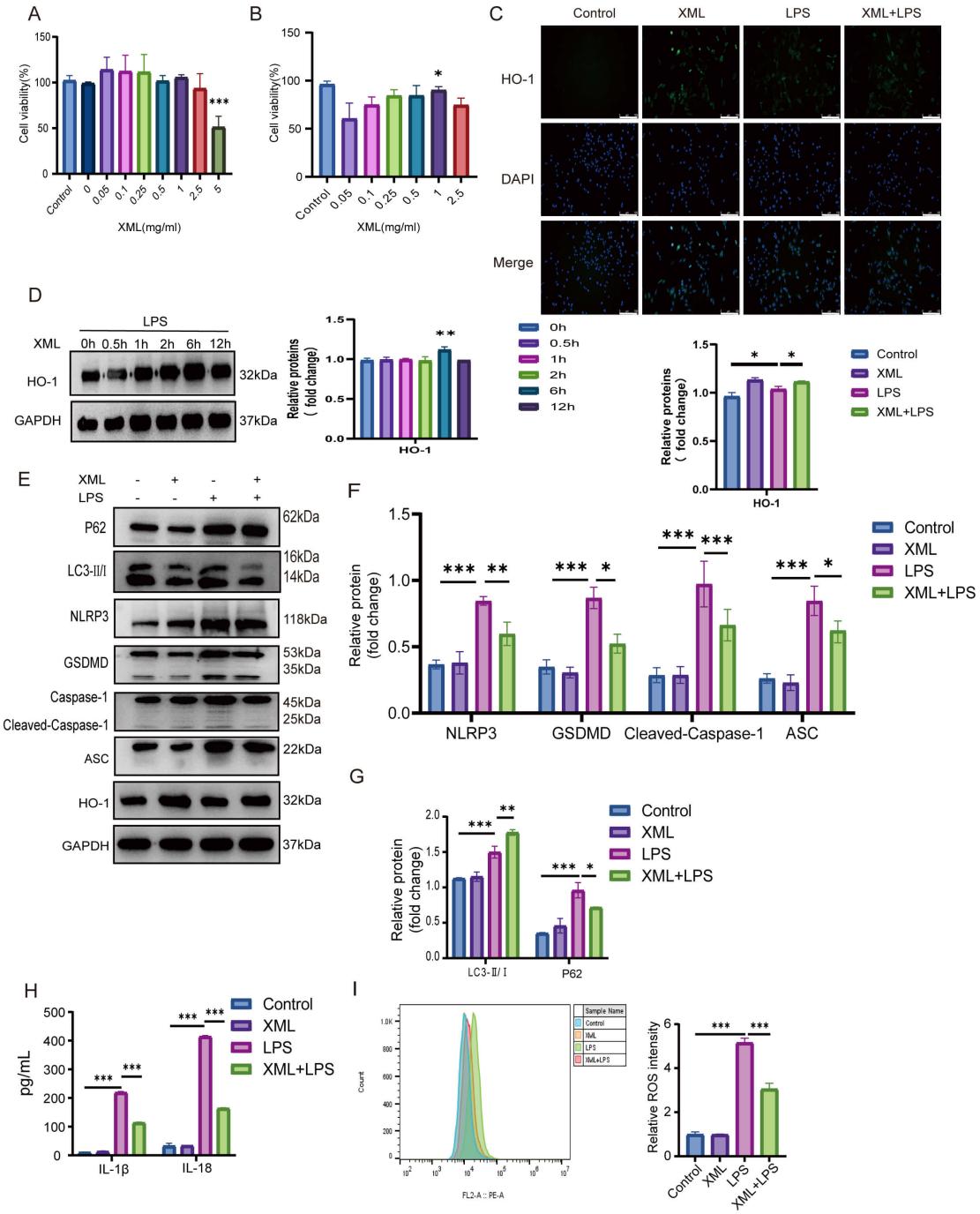


Fig. 3. XML promotes autophagy and reduces inflammation and pyroptosis. (A) The effect of XML on the viability of HL-1 cells was assessed using the CCK-8 assay (n = 6). (B) HL-1 cells were stimulated with a fixed concentration of LPS (Control group is an LPS-only group), and the effect of XML on cell viability was evaluated by CCK-8 assay (n = 6). (C–E) HO-1 expression analysis. The expression of HO-1 in HL-1 cells was analyzed by Western blot and immunofluorescence (scale bar: 100 μm), and the time-dependent effects of XML on HO-1 expression were determined. Protein levels were quantified by gray-scale analysis and normalized to GAPDH (n = 3). (F,G) Inflammasome-related protein analysis. Proteins were extracted from HL-1 cells, and the expression levels of inflammasome-related proteins (NLRP3, GSDMD, cleaved caspase-1, ASC, P62, LC3-II/I) associated with pyroptosis were analyzed by Western blot. Protein levels were quantified by gray-scale analysis and normalized to GAPDH (n = 3). (H) Inflammatory cytokines IL-1β and IL-18 in the cell supernatant were detected by ELISA (n = 6). (I) ROS levels in different groups of cells were measured using the DHE kit (n = 6). $^{*}p < 0.05$, $^{**}p < 0.01$, $^{***}p < 0.001$. ROS, reactive oxygen species; DHE, dihydroethidium.

the effect of XML on autophagy in SIMD, the expression of autophagy-related proteins LC3 and P62 was examined. The results showed that LC3-II/I expression was significantly upregulated, whereas P62 expression was markedly downregulated in the LPS+XML group compared with the LPS group (Fig. 2A,F), indicating enhanced autophagosome formation in cardiac tissue.

3.3 XML Promotes Autophagy and Reduces Inflammation and Pyroptosis

Previous studies have demonstrated that HL-1 cells activate various signaling cascades, such as cytokine production and oxidative stress, upon LPS exposure, making HL-1 a suitable model for investigating SIMD [21,22,23]. To explore the underlying mechanisms of XML, HL-1 cells were pretreated with XML, followed by LPS stimulation. Cell viability assays showed that XML treatment significantly increased cell viability (Fig. 3A,B).

Pretreatment at different time points revealed that HO-1 expression was highest when XML was added 6 hours in advance. Therefore, 6 hours was chosen as the optimal pretreatment time. To investigate the effects of XML on autophagy and pyroptosis in HL-1, cells were treated with XML and LPS. The results showed that XML significantly upregulated HO-1 expression and downregulated NLRP3, ASC, caspase-1, and GSDMD expression compared with the LPS group. Western blot analysis revealed that XML facilitated the conversion of LC3-II/I and reduced the accumulation of P62 (Fig. 3C–G). Furthermore, XML treatment significantly reduced IL-1β and IL-18 levels in LPS-stimulated HL-1 cells, as shown by ELISA (Fig. 3H).

As reported in previous studies, intraperitoneal LPS administration alters antioxidant enzyme activity and increases oxidative stress markers in cardiac tissue [24]. DHE fluorescence was used to measure ROS levels. The results showed that ROS levels were significantly higher in the LPS group compared to the control group. However, XML treatment significantly reduced ROS levels, suggesting that XML alleviates LPS-induced oxidative stress in myocardial cells (Fig. 3I).

3.4 HO-1 Regulates the Effects of XML on LPS-Induced Myocardial Injury

To verify whether XML exerts cardioprotective effects against LPS-triggered cardiomyocyte injury via the HO-1 signaling axis, we employed ZnPP, a selective HO-1 inhibitor. Functional and molecular data revealed that ZnPP pretreatment abrogated the beneficial actions of XML. Specifically, ZnPP reversed the protective effects of XML on LPS-induced pyroptosis-related proteins, such as NLRP3, GSDMD, and ASC. Moreover, the modulatory effects of XML on LC3-I to LC3-II conversion and P62 clearance were also abolished following ZnPP intervention (Fig. 4A,B); meanwhile, it further reversed the effect of XML on the release of inflammatory mediators of IL-1β and IL-18 (Fig. 4C).

3.5 Autophagy Mediates the Effect of XML on LPS-Induced Pyroptosis

The interaction between autophagy and pyroptosis in HL-1 cells after LPS treatment with XML was assessed by the autophagy inhibitor 3-methyladenine (3-MA). The results showed that 3-MA treatment reversed the effect of XML on the expression of HO-1, LC3-I to LC3-II conversion and P62. Moreover, 3-MA treatment also reversed the inhibitory effect of XML on NLRP3, ASC, and GSDMD expression in LPS-treated HL-1 cells (Fig. 5A–D). Consistent ELISA results further revealed increased secretion of IL-1β and IL-18 (Fig. 5E). Collectively, these findings indicated that 3-MA abrogates XML's inhibitory effect on LPS-triggered pyroptotic signaling in cardiomyocytes. In HL-1 cells with LPS-induced injury, parallel experiments further validated that XML suppresses NLRP3 expression and reduces ROS accumulation via upregulating HO-1 expression (Fig. 5F).

4. Discussion

XML is a bioactive extract derived from the *Periplaneta americana*, which exhibits cardioprotective, microcirculatory improvement, and diuretic effects [12,25]. Previous studies have demonstrated that XML improves myocardial function in heart failure rats and attenuates myocardial ischemia-reperfusion injury [14,26,27]. However, the specific mechanism underlying the protective effect of XML against SIMD remains unclear. The present study demonstrates that XML pretreatment significantly improves survival and cardiac function in LPS-induced SIMD mice, and that this cardioprotection is associated with HO-1 activation, autophagy induction, and pyroptosis inhibition.

Cardiac performance was assessed by echocardiography in mice. Our results showed that XML pretreatment increased survival in LPS-challenged mice with sepsis-induced myocardial dysfunction. Echocardiography showed that LPS administration decreased LVEF and LVFS, indicating cardiac dysfunction. XML treatment significantly improved cardiac function and reduced myocardial damage biomarkers, including CK and LDH. These results are consistent with previous reports demonstrating that XML protects against ischemia-reperfusion injury and myocardial infarction.

This study investigated the effects of XML on inflammatory responses and pyroptotic processes in SIMD using both *in vitro* and *in vivo* models. It was shown that XML treatment reduced NLRP3 inflammasome activation and pyroptosis in HL-1 cells and cardiac tissues in the LPS model. The present results show that XML inhibited NLRP3, ASC, caspase-1, and GSDMD expression and reduced IL-1β and IL-18 secretion. The reduction in pyroptosis is consistent with HO-1 pathway activation, which has been shown to reduce NLRP3 inflammasome activation and pyroptosis in cardiomyocytes.

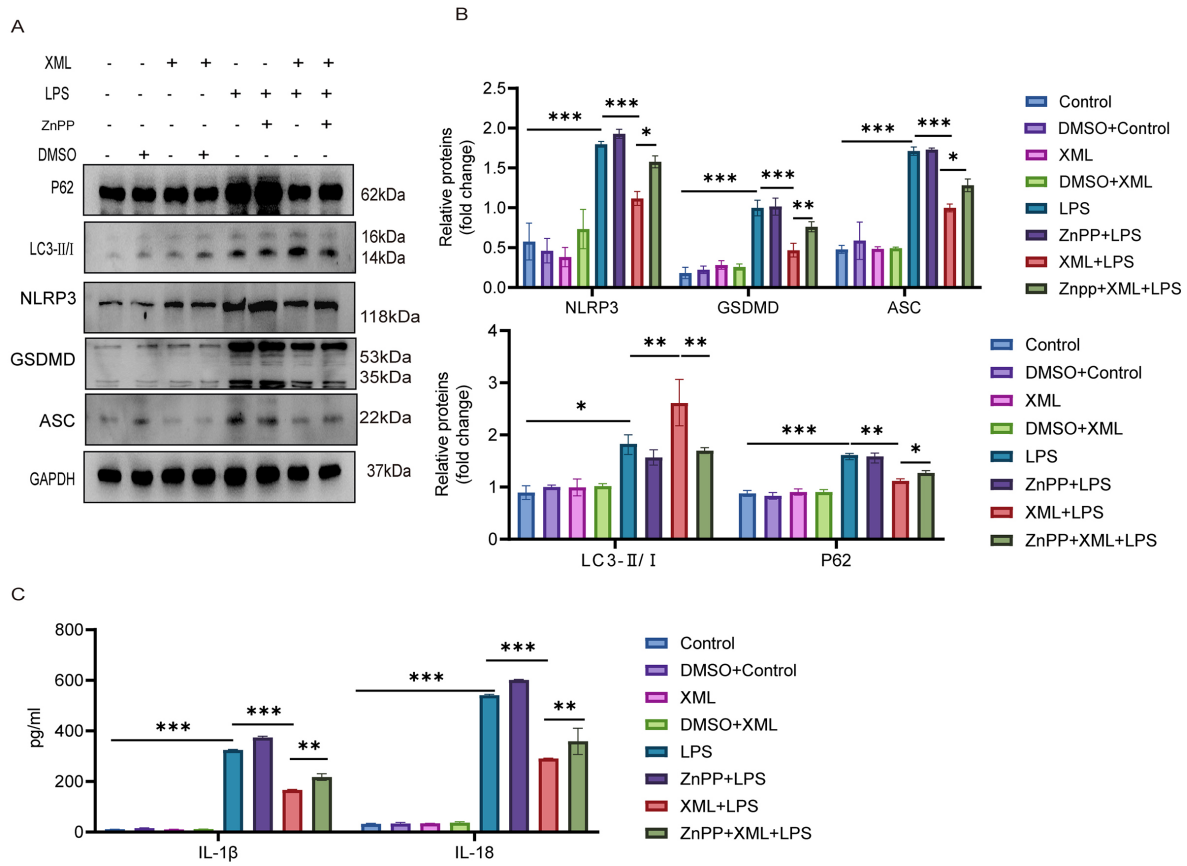


Fig. 4. HO-1 regulates the effects of XML on LPS-induced myocardial injury. (A,B) Western blot was performed to detect the expression of pyroptosis-associated inflammasome proteins (NLRP3, ASC, GSDMD), and LC3-II/I, P62 in HL-1 cells. Band gray-scale quantification was conducted with signals normalized to GAPDH (n = 3). (C) Secreted IL-1β and IL-18 in cell culture supernatants were quantified via ELISA (n = 6). $^{*}p < 0.05$, $^{**}p < 0.01$, $^{***}p < 0.001$.

Autophagy is a cellular degradation mechanism involving sequestration of misfolded proteins and damaged organelles within autophagosomes, which then fuse with lysosomes to form autolysosomes for degradation [28,29]. The role of autophagy in SIMD is complex. Some studies have shown that autophagy protects against sepsis-induced cardiac dysfunction by removing damaged mitochondria and reducing ROS production. However, other studies have shown that excessive autophagy can lead to cell death and worsen cardiac function in sepsis. The present results show that XML upregulated LC3-II/I expression and downregulated P62 expression, indicating that XML promotes autophagy. This increase in autophagy is associated with reduced pyroptosis and oxidative stress, which is consistent with previous reports that autophagy protects against sepsis-induced cardiac dysfunction by reducing inflammation and oxidative stress [30,31,32,33].

LPS stimulation significantly enhances ROS generation in cells [34]. The excessive production of ROS disrupts redox balance, leading to pyroptosis and ultimately exacerbating myocardial injury and cardiac dysfunction [35,36,37]. Our results show that XML reduced ROS in LPS-treated HL-1 cells, indicating its antioxidant effects. The antioxidant effect of XML is associated with HO-1 activation, a key enzyme in the antioxidant defense system. HO-1 activation increases bilirubin and carbon monoxide production, both of which exert antioxidant and anti-inflammatory effects. However, few studies have reported the correlation between XML-mediated alleviation of oxidative stress and HO-1 activity.

Previous studies have established the individual roles of HO-1/Nrf2, NLRP3 inflammasome, ROS, and autophagy in septic cardiomyopathy [38]. Our work demonstrated that XML simultaneously regulates the above signaling cascades by restoring autophagy alongside HO-1 upregulation. Our experiments with the autophagy inhibitor 3-MA further confirmed that XML blocks pyroptosis relies in part on its capacity to boost autophagy. Furthermore, using ZnPP to inhibit HO-1 activity attenuated XML's suppression of NLRP3 inflammasome and GSDMD cleavage, indicating that the anti-pyroptotic effect of XML is partially dependent on HO-1 activation. Collectively, our findings establish a novel mechanistic model connecting HO-1, autophagy and pyroptosis to explain how XML alleviates LPS-mediated SIMD.

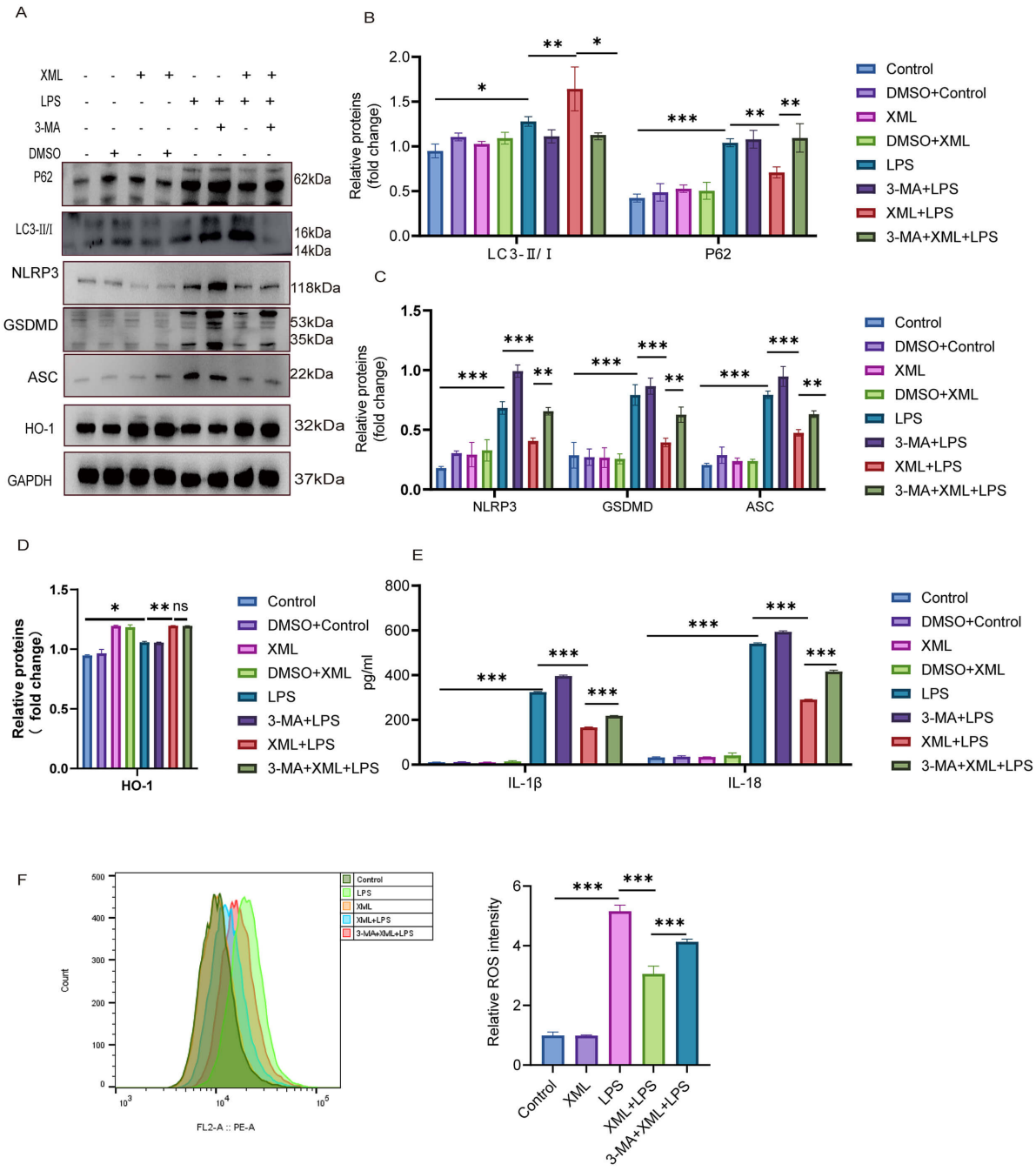


Fig. 5. The effect of autophagy-regulated XML on pyroptosis induced by LPS. (A–D) Proteins were extracted from HL-1 cells, and the expression levels of autophagy-related LC3-II/I, P62 and inflammasome-related proteins (NLRP3, GSDMD, ASC) associated with pyroptosis, and HO-1 were analyzed by Western blot. Protein levels were quantified using gray-scale analysis and normalized to GAPDH (n = 3). (E) Inflammatory cytokines IL-1β and IL-18 in the cell supernatant were detected by ELISA (n = 6). (F) ROS levels in different groups of cells were measured using the DHE kit (n = 6). Pilot experiments confirmed that neither DMSO nor 3-MA alone significantly affected pyroptosis in HL-1 cells. Therefore, to maintain clarity and focus on the mechanistic interplay, these groups were omitted from the main figure. ns, not significant. $^{*}p < 0.05$, $^{**}p < 0.01$, $^{***}p < 0.001$.

A limitation of this study is that HO-1 was inhibited only pharmacologically, which lacks complete specificity and may interfere with other heme-related pathways. Therefore, without genetic validation, the effects of XML in SIMD are mediated primarily by HO-1 remains preliminary. Furthermore, this study utilized only HL-1 cells and an LPS-induced mouse model of SIMD, which may not fully recapitulate the complexity of clinical sepsis. Therefore, future studies should include more specific genetic manipulations and diverse animal models to confirm the

central role of HO-1 in the cardioprotective effect of XML. Although our preclinical findings support the cardioprotective potential of XML against SIMD, the present study is limited to *in vitro* cardiomyocyte and LPS-induced animal models. Further clinical evidence is needed to validate the efficacy and safety of XML in septic patients with cardiac dysfunction.

5. Conclusion

Collectively, our findings demonstrate that XML confers myocardial protection against SIMD through coordinated modulation of the NLRP3 inflammasome pyroptosis axis, mechanistically linked to its participation in HO-1-mediated autophagy and antioxidant defense. These insights establish XML as a promising therapeutic candidate for sepsis-induced cardiac dysfunction, warranting further translational investigation.

Availability of Data and Materials

The data that support the findings of this study are available from the corresponding authors upon reasonable request.

Author Contributions

YZX and LLY designed the research study. YJL and WX performed the research. YT wrote the manuscript. SYL and YT conducted experiments. YT, YJ, TC, and XXG analyzed the data. All authors contributed to editorial changes in the manuscript. All authors read and approved the final manuscript. All authors have participated sufficiently in the work and agreed to be accountable for all aspects of the work.

Ethics Approval and Consent to Participate

All animal procedures were approved by the Institutional Animal Care and Use Committee in Hunan Provincial People's Hospital (Approval Number No. 69/2023). All animal experimental protocols followed the National Standards for Laboratory Animal Welfare set up by the Ministry of Science and Technology of China. The study was carried out in accordance with the ARRIVE guidelines.

Acknowledgment

Not applicable.

Funding

This work was financially supported by grants from the Hunan Province Natural Science Foundation (Grant No.2022JJ80062, 2024JJ9289, 2024JJ8203, 2025JJ80746, 2024JJ8145), the Hunan Provincial Health Commission Scientific Research Project (W20243096), Project of Changsha Natural Science Foundation (kq2403138).

Conflicts of Interest

The authors declare no conflicts of interest.

Supplementary Material

Supplementary material associated with this article can be found, in the online version, at https://doi.org/10.31083/FBL52450.

References

[1] Martin-Loeches I, Singer M, Leone M. Sepsis: key insights, future directions, and immediate goals. A review and expert opinion. Intensive Care Medicine. 2024; 50: 2043–2049. https://doi.org/10.1007/s00134-024-07694-z

[2] Yu X, Gao J, Zhang C. Sepsis-induced cardiac dysfunction: mitochondria and energy metabolism. Intensive Care Medicine Experimental. 2025; 13: 20. https://doi.org/10.1186/s40635-025-00728-w

[3] Tang Y, Wu J, Sun X, Tan S, Li W, Yin S, et al. Cardiolipin oxidized by ROS from complex II acts as a target of gasdermin D to drive mitochondrial pore and heart dysfunction in endotoxemia. Cell Reports. 2024; 43: 114237. https://doi.org/10.1016/j.celrep.2024.114237

[4] Song C, Zhang Y, Pei Q, Zheng L, Wang M, Shi Y, et al. HSP70 alleviates sepsis-induced cardiomyopathy by attenuating mitochondrial dysfunction-initiated NLRP3 inflammasome-mediated pyroptosis in cardiomyocytes. Burns & Trauma. 2022; 10: tkac043. https://doi.org/10.1093/burnst/tkac043

[5] Zhang Y, Lv Y, Zhang Q, Wang X, Han Q, Liang Y, et al. ALDH2 attenuates myocardial pyroptosis through breaking down Mitochondrion-NLRP3 inflammasome pathway in septic shock. Frontiers in Pharmacology. 2023; 14: 1125866. https://doi.org/10.3389/fphar.2023.1125866

[6] Joshi S, Kundu S, Priya VV, Kulhari U, Mugale MN, Sahu BD. Anti-inflammatory activity of carvacrol protects the heart from lipopolysaccharide-induced cardiac dysfunction by inhibiting pyroptosis via NLRP3/Caspase1/Gasdermin D signaling axis. Life Sciences. 2023; 324: 121743. https://doi.org/10.1016/j.lfs.2023.121743

[7] Nagar A, Rahman T, Harton JA. The ASC Speck and NLRP3 Inflammasome Function Are Spatially and Temporally Distinct. Frontiers in Immunology. 2021; 12: 752482. https://doi.org/10.3389/fimmu.2021.752482

[8] Dai R, Ren Y, Lv X, Chang C, He S, Li Q, et al. MicroRNA-30e-3p reduces coronary microembolism-induced cardiomyocyte pyroptosis and inflammation by sequestering HDAC2 from the *SMAD7* promoter. American Journal of Physiology. Cell Physiology. 2023; 324: C222–C235. https://doi.org/10.1152/ajpcell.00351.2022

[9] Wang SH, Cui LG, Su XL, Komal S, Ni RC, Zang MX, et al. GSK-3β-mediated activation of NLRP3 inflammasome leads to pyroptosis and apoptosis of rat cardiomyocytes and fibroblasts. European Journal of Pharmacology. 2022; 920: 174830. https://doi.org/10.1016/j.ejphar.2022.174830

[10] Han X, Chen X, Liu Y, Yang J, Nie W, Yang M, et al. Xinmailong injection on left ventricular remodeling and inflammatory mediators in patients with CHF: a systematic review and meta-analysis. Frontiers in Pharmacology. 2024; 15: 1370448. https://doi.org/10.3389/fphar.2024.1370448

[11] Qi J, Yu J, Tan Y, Chen R, Xu W, Chen Y, et al. Mechanisms of Chinese Medicine Xinmailong's protection against heart failure in pressure-overloaded mice and cultured cardiomyocytes. Scientific Reports. 2017; 7: 42843. https://doi.org/10.1038/srep42843

[12] He J, Zhao X, Lin X, Yang Z, Ma M, Ma L, et al. The Effect of Xinmailong Infusion on Sepsis-Induced Myocardial Dys-

function: a Pragmatic Randomized Controlled Trial. Shock (Augusta, Ga.). 2021; 55: 33–40. https://doi.org/10.1097/SHK.0000000000001592

[13] Jin L, Yin Q, Mao Y, Gao Y, Han Q, Mei R, et al. Putative Prevention of XML Injection Against Myocardial Ischemia Is Mediated by PKC and PLA2 Proteins. Frontiers in cell and developmental biology. 2022; 10: 827691. https://doi.org/10.3389/fcell.2022.827691

[14] Jiang Y, Liu Y, Xiao W, Zhang D, Liu X, Xiao H, et al. Xinmailong Attenuates Doxorubicin-Induced Lysosomal Dysfunction and Oxidative Stress in H9c2 Cells via HO-1. Oxidative Medicine and Cellular Longevity. 2021; 2021: 5896931. https://doi.org/10.1155/2021/5896931

[15] Fallach R, Shainberg A, Avlas O, Fainblut M, Chepurko Y, Porat E, et al. Cardiomyocyte Toll-like receptor 4 is involved in heart dysfunction following septic shock or myocardial ischemia. Journal of Molecular and Cellular Cardiology. 2010; 48: 1236–1244. https://doi.org/10.1016/j.yjmcc.2010.02.020

[16] Luo M, Peng Y, Lv D, Xue Y, Huang L, Hu Y, et al. LncRNA GAS5 downregulates NLRP3 inflammasome activation-mediated pyroptosis in sepsis-induced myocardial injury by targeting SIRT3/AMPKα. Heliyon. 2023; 9: e22939. https://doi.org/10.1016/j.heliyon.2023.e22939

[17] Gao X, Ruan X, Ji H, Peng L, Qiu Y, Yang D, et al. Maduramicin triggers methuosis-like cell death in primary chicken myocardial cells. Toxicology Letters. 2020; 333: 105–114. https://doi.org/10.1016/j.toxlet.2020.07.025

[18] Chen D, Jin Z, Zhang J, Jiang L, Chen K, He X, et al. HO-1 Protects against Hypoxia/Reoxygenation-Induced Mitochondrial Dysfunction in H9c2 Cardiomyocytes. PloS One. 2016; 11: e0153587. https://doi.org/10.1371/journal.pone.0153587

[19] Lei L, Chai Y, Lin H, Chen C, Zhao M, Xiong W, et al. Dihydroquercetin Activates AMPK/Nrf2/HO-1 Signaling in Macrophages and Attenuates Inflammation in LPS-Induced Endotoxemic Mice. Frontiers in Pharmacology. 2020; 11: 662. https://doi.org/10.3389/fphar.2020.00662

[20] Lei Y, Zhou R, Sun X, Tang F, Gao H, Chen L, et al. The pannexin-1 channel regulates pyroptosis through autophagy in a mouse model of sepsis-associated encephalopathy. Annals of Translational Medicine. 2021; 9: 1802. https://doi.org/10.21037/atm-21-6579

[21] Yang Z, Pan X, Wu X, Lin Q, Chen Y, Cai S, et al. TREM-1 induces pyroptosis in cardiomyocytes by activating NLRP3 inflammasome through the SMC4/NEMO pathway. The FEBS Journal. 2023; 290: 1549–1562. https://doi.org/10.1111/febs.16644

[22] Yu Z, Xiao Z, Guan L, Bao P, Yu Y, Liang Y, et al. Translocation of gasdermin D induced mitochondrial injury and mitophagy mediated quality control in lipopolysaccharide related cardiomyocyte injury. Clinical and Translational Medicine. 2022; 12: e1002. https://doi.org/10.1002/ctm2.1002

[23] Gong X, Li Y, He Y, Zhou F. USP7-SOX9-miR-96-5p-NLRP3 Network Regulates Myocardial Injury and Cardiomyocyte Pyroptosis in Sepsis. Human Gene Therapy. 2022; 33: 1073–1090. https://doi.org/10.1089/hum.2022.078

[24] Wang C, Han D, Feng X, Hu L, Wu J. Docosahexaenoic acid alleviates LPS-induced cytotoxicity in HL-1 cardiac cells via improving stress-induced mitochondrial fragmentation. Heliyon. 2023; 9: e22465. https://doi.org/10.1016/j.heliyon.2023.e22465

[25] Wang H, Ye Y, Wan W, Wang L, Li R, Li L, et al. Xinmailong Modulates Platelet Function and Inhibits Thrombus Formation *via* the Platelet αIIbβ3-Mediated Signaling Pathway. Frontiers in Pharmacology. 2019; 10: 923. https://doi.org/10.3389/fphar.2019.00923

[26] Jing-Jing W, Ming-Jun Z, Yong-Xia W, Bin LI, Guang-Cao P, Xin-Lu W, et al. Systematic review of efficacy and safety of Xinmailong Injection in treatment of coronary heart disease complicated with heart failure. Zhongguo Zhong Yao Za Zhi = Zhongguo Zhongyao Zazhi = China Journal of Chinese Materia Medica. 2020; 45: 4756–4765. https://doi.org/10.19540/j.cnki.cjcmm.20200302.505

[27] Xue Y, Lv C, Jin L, Tan D, Wu D, Peng I. Study on the mechanism of Xinmailong injection against chronic heart failure based on transcriptomics and proteomics. Journal of Pharmaceutical and Biomedical Analysis. 2025; 253: 116529. https://doi.org/10.1016/j.jpba.2024.116529

[28] Jiang Y, Xu J, Zeng H, Lin Z, Yi Q, Guo J, et al. miR-29b-1-5p exacerbates myocardial injury induced by sepsis in a mouse model by targeting TERF2. Acta Biochimica et Biophysica Sinica. 2024; 56: 607–620. https://doi.org/10.3724/abbs.2024020

[29] Han D, Wang C, Feng X, Hu L, Wang B, Hu X, et al. ALCAT1-Mediated Pathological Cardiolipin Remodeling and PLSCR3-Mediated Cardiolipin Transferring Contribute to LPS-Induced Myocardial Injury. Biomedicines. 2024; 12: 2013. https://doi.org/10.3390/biomedicines12092013

[30] Yuan H, Perry CN, Huang C, Iwai-Kanai E, Carreira RS, Glembotski CC, et al. LPS-induced autophagy is mediated by oxidative signaling in cardiomyocytes and is associated with cytoprotection. American Journal of Physiology. Heart and Circulatory Physiology. 2009; 296: H470–H479. https://doi.org/10.1152/ajpheart.01051.2008

[31] Ikeda S, Zablocki D, Sadoshima J. The role of autophagy in death of cardiomyocytes. Journal of Molecular and Cellular Cardiology. 2022; 165: 1–8. https://doi.org/10.1016/j.yjmcc.2021.12.006

[32] Zhang E, Zhao X, Zhang L, Li N, Yan J, Tu K, et al. Minocycline promotes cardiomyocyte mitochondrial autophagy and cardiomyocyte autophagy to prevent sepsis-induced cardiac dysfunction by Akt/mTOR signaling. Apoptosis : an International Journal on Programmed Cell Death. 2019; 24: 369–381. https://doi.org/10.1007/s10495-019-01521-3

[33] Wu B, Song H, Fan M, You F, Zhang L, Luo J, et al. Luteolin attenuates sepsis-induced myocardial injury by enhancing autophagy in mice. International Journal of Molecular Medicine. 2020; 45: 1477–1487. https://doi.org/10.3892/ijmm.2020.4536

[34] Li Y, Feng YF, Liu XT, Li YC, Zhu HM, Sun MR, et al. Songorine promotes cardiac mitochondrial biogenesis via Nrf2 induction during sepsis. Redox Biology. 2021; 38: 101771. https://doi.org/10.1016/j.redox.2020.101771

[35] Zeng H, Zou P, Chen Y, Zhang P, Shao L. NOX4 aggravates doxorubicin-induced cardiomyocyte pyroptosis by increasing reactive oxygen species content and activating the NLRP3 inflammasome. Cardiovascular Diagnosis and Therapy. 2024; 14: 84–100. https://doi.org/10.21037/cdt-23-142

[36] Marconi GD, Della Rocca Y, Fonticoli L, Guarnieri S, Carradori S, Rajan TS, et al. The Beneficial Effect of Carvacrol in HL-1 Cardiomyocytes Treated with LPS-G: Anti-Inflammatory Pathway Investigations. Antioxidants (Basel, Switzerland). 2022; 11: 386. https://doi.org/10.3390/antiox11020386

[37] Mandaglio-Collados D, Ruiz-Alcaraz AJ, Rivera-Caravaca JM, Ramos-Bratos MP, Marín F, López-Gálvez R. Analysis of key proinflammatory mechanisms in cardiovascular pathology through stimulation with lipopolysaccharide and urban particulate matter in mouse atrial cardiomyocytes. Environmental Toxicology and Pharmacology. 2025; 114: 104652. https://doi.org/10.1016/j.etap.2025.104652

[38] Rahim I, Sayed RK, Fernández-Ortiz M, Aranda-Martínez P, Guerra-Librero A, Fernández-Martínez J, et al. Melatonin alleviates sepsis-induced heart injury through activating the Nrf2 pathway and inhibiting the NLRP3 inflammasome. Naunyn-Schmiedeberg's archives of Pharmacology. 2021; 394: 261–277. https://doi.org/10.1007/s00210-020-01972-5